Distinguishing the local environments of Ga and Ge in amorphous (Ga 2 Se 3) 0.25 (GeSe 2) 0.75 by anomalous x-ray scattering

B D Klee, J R Stellhorn, M Krbal, N. Boudet, G. Chahine, Nils Blanc, W C Pilgrim, T Wagner, S Hosokawa

HAL Id: hal-01957293
https://hal.science/hal-01957293

DISTINGUISHING THE LOCAL ENVIRONMENTS OF Ga AND Ge IN AMORPHOUS (Ga₂Se₃)₀.₂₅(GeSe₂)₀.₇₅ BY ANOMALOUS X-RAY SCATTERING

B. D. KLEE[a*], J. R. STELLHORN[a,b], M. KRBAL[c], N. BOUDET[d],
G. A. CHAHINE[e], N. BLANC[d], W. C. PILGRIM[a], T. WAGNER[c,f],
S. HOSOKAWA[a,b]

[a]*Physical Chemistry Department, Philipps-University, Hans-Meerwein Str. 4, 35032 Marburg, Germany*
[b]*Department of Physics, Kumamoto University, Kumamoto 860-8555, Japan*
[c]*Center of Materials and Nanotechnologies, Faculty of Chemical Technology, University of Pardubice, Nam. Cs. Legii 565, 53210 Pardubice, Czech Republic*
[d]*CNRS, Université Grenoble Alpes, Institut Néel, 38000 Grenoble, France*
[e]*CNRS, Université Grenoble Alpes, Grenoble INP, SIMAP, 38000 Grenoble, France*
[f]*Department of General and Inorganic Chemistry, Faculty of Chemical Technology, University of Pardubice, Studentska 573, 53210 Pardubice, Czech Republic*

The amorphous structure of $(Ga_2Se_3)_{0.25}(GeSe_2)_{0.75}$ is investigated using a combination of anomalous X-ray scattering (AXS) and Reverse-Monte-Carlo (RMC) modeling. It was confirmed that the Ga and Ge atoms can be found exclusively in the tetrahedral configuration. The average coordination number of the Se atoms is found to be 2.34(3) due to the presence of dative bonds. The formation of Ga/Ge-Ga/Ge so-called "wrong bonds" is discussed based on a set of RMC simulations. A strong Ga-Ga second neighbor correlations indicates the formation of Ga-Se clusters within the Ga-Ge-Se glass.

1. Introduction

Chalcogenide glasses exhibit many interesting properties. Among them, infrared transparency and a high optical nonlinearity offer many potential applications in infrared optics and optoelectronics. [1-4] Since the high glass forming ability of many chalcogenide glasses is very good the composition can be varied in a wide range of element concentrations, which makes it possible to tune specific properties of these glasses. For example the incorporation of Ga in $GeSe_2$ was shown to increase the solubility of rare earth elements such as Er in the glass, which enables a huge range of accessible properties. [5,6] Since the physical properties are tightly linked to the structure (structural units) of the amorphous phase, the structure of chalcogenide glasses have been investigated for several decades. In the case of amorphous Ga-Ge-Se glasses it is not simple to differentiate between gallium and germanium, since the neutron scattering lengths b as well as the X-ray form factors f are very similar for both elements. In the last years multiple similar compositions of such Ga-Ge-Se glasses were investigated using Extended X-ray Absorption Fine Structure spectroscopy (EXAFS) [7,8], optical and Raman spectroscopy [9,10], X-ray photoelectron spectroscopy (XPS) [7], neutron scattering [8], and advanced nuclear resonance spectroscopy (NMR) techniques [11]. Each of these methods is either limited to nearest neighbor information, or lacks contrast to reliably differentiate between similar elements and will

---

*Corresponding author: benjamin.klee@staff.uni-marburg.de

mostly yield averaged information. In contrast, Anomalous X-ray Scattering (AXS) combines the advantages of scattering methods, which is information about the nearest neighbor as well as intermediate range order, and element specific methods.[12-16] Here, we demonstrate a combination of AXS and RMC as an effective tool to provide structural information about the $Ga_{14.3}Ge_{21.4}Se_{64.3}$ glass, which is a composition on the pseudobinary tie-line $(Ga_2Se_3)_x(GeSe_2)_{1-x}$ where x=0.25.

2. Experimental

A total 5 g of pure elements were placed into a quartz ampoule, evacuated to 10^{-4} Pa and sealed. Next, the ampoule was placed to a rocking furnace to 1050°C (rate 1° C/min) and then kept rocking for 12h at this temperature. In a further step the temperature was reduced to 850° C (2° C/min), then stop rocking for 1h and subsequently the ampoule was quenched in cold water for about 10s. The sample was immediately annealed at 350° C for 3h and then gradually cooled to room temperature. The resulting bulk was polished and the bulk composition was confirmed at multiple sample positions by Energy-dispersive X-ray spectroscopy (EDXS) at 30 kV electron energy. The scattering experiments were performed at the ESRF BM02 using a highly monochromatic primary beam in reflection geometry. Differential structure factors ΔS(q) were obtained using a 2D detection system coupled with an analyzer crystal. The beam energies were chosen to be 20 eV or 200 eV below the corresponding K-alpha absorption edge for the near and far edge measurements respectively. The total structure factor S(q) was measured at 17.008 keV and a scintillation point detector coupled with the same analyzer crystal and a slit system were used in this case. The weighting factors for these measurements at the structure factor maximum $Q=2$ Å^{-1} as well as for neutron scattering are shown in table 1. It can be seen that the information density of X-ray and neutron total scattering functions is small for correlations containing only Ga and Ge. The differential structure factors exhibit increased weighting factors for all correlations including the respective element. This way, different correlations can be distinguished more accurately by introducing a contrast between multiple scattering experiments.

Table 1: Weighting factors for all experimental structure factors at $Q=2$ Å^{-1} and neutron scattering.

energy	w_{Ga-Ga}	w_{Ga-Ge}	w_{Ga-Se}	w_{Ge-Ge}	w_{Ge-Se}	w_{Se-Se}
17 keV	0.018	0.057	0.178	0.043	0.273	0.430
Se-far	0.021	0.064	0.184	0.049	0.279	0.403
ΔGa	0.096	0.177	0.555	0.020	0.086	0.067
ΔGe	-0.011	0.117	-0.039	0.180	0.675	0.077
ΔSe	-0.001	-0.005	0.149	-0.004	0.220	0.641
Neutron Scattering	0.017	0.058	0.170	0.049	0.286	0.419

The high Energy structure factor, as well as the Se-far and all differential structure factors were fitted simultaneously using Reverse-Monte-Carlo modeling (RMC).[17] The sample density is assumed to be 4.417 g/cm^3 (taken from [10]). Our RMC simulations proceeded as follows: Firstly, a random configuration containing 20300 atoms was generated and equilibrated by simulating without including experimental datasets. This configuration was used as a starting point for further simulations. The minimum interatomic distance was chosen to be 2 Å from this point on. A model simulation was performed without excluding any bonds. In the next step, different bonds were forbidden by changing the proper minimum distance to 2.9 Å while changes in the quality of fit are monitored in the form of R_w values, which are related to χ^2 from comparing the simulated structure factors with the experimental data (see [18] for more information on the exact definition of R_w). Low R_w values correlate to a good agreement of experiment and simulation. In these simulations atoms were moved a total of $3·10^7$ times with an acceptance rate of roughly 28%.

3. Results and discussion

The results of several simulations with different combinations of excluded bonds are summarized in table 2. The average R_w value, showing the quality of the fit, represents the average of the R_w values of all fitted experimental datasets. From each simulation dataset the generalized 8-N rule value is calculated following [19] and is expected to be 8. When excluding any Se bond the experimental data could not be reproduced, therefore no such simulation is discussed further. The following discussion will focus on so-called "wrong bonds" (Ga/Ge-Ga/Ge). The simulations presented here can be divided into two groups: Whenever Ga or Ge were not allowed to form bonds to any other Ga or Ge atom, which is the case for simulations 5 and 7, the R_w value increased. In these simulations the general 8-N rule is less satisfied than in all others. Additionally, the averaged coordination numbers calculated from these simulations are significantly different compared to other simulations. These effects are weaker when constraining Ga (simulation 5), since the low Ga amount in the sample limits the information content of this element in the scattering data. Therefore the interpretation will focus on simulations 1 to 4 and 6. These simulations are very similar regarding their results.

Table 2. Total coordination numbers (CN) acquired from simulations with different combinations of excluded bonds. Each forbidden bond is marked with X

Sim No.	Ga-Ga	Ga-Ge	Ge-Ge	CN Ga	CN Ge	CN Se	average R_w / %	8-N rule
1				4.08	3.99	2.33	6.14	8.09
2	X			3.97	3.99	2.34	6.12	8.12
3		X		4.06	3.98	2.32	6.19	8.10
4			X	4.13	3.86	2.34	6.18	8.14
5	X	X		3.51	3.98	2.36	6.57	8.26
6	X		X	4.03	3.86	2.35	6.16	8.17
7		X	X	3.83	3.05	2.45	8.51	8.58

The simulations imply that the presence of wrong bonds for both Ga and Ge is supported by the presented data. Since excluding single bonds does not have a significant impact on the overall structure or the fit quality, Ga and Ge seem to play a similar role in the structure formation and are mostly interchangeable without change in the short range order. Partial coordination numbers obtained from the simulations are shown in table 3.

Table 3. Partial coordination numbers obtained in different simulations

Sim No.	1	2	3	4	6
Ga-Ga	0.52	-	0.97	0.52	-
Ga-Ge	0.88	1.05	-	1.22	1.31
Ga-Se	2.68	2.91	3.09	2.39	2.71
Ge-Ga	0.59	0.70	-	0.81	0.87
Ge-Ge	0.83	0.83	1.25	-	-
Ge-Se	2.57	2.46	2.73	3.04	2.99
Se-Ga	0.60	0.65	0.69	0.53	0.60
Se-Ge	0.86	0.82	0.91	1.01	1.00
Se-Se	0.88	0.87	0.73	0.80	0.75

We find that, on average, Ga and Ge form 1-1.5 wrong bonds while the Se-Se coordination number is 0.8±0.1. We decided to proceed with the simulation that combines both, lowest R_w value and highest number of constraints, which is simulation 6 in this case. The partial coordination numbers from this simulation are comparable to those obtained by Pethes et. al. for a similar composition ($Ga_{10}Ge_{20}Se_{70}$), who excluded the same combination of bonds.[8] For simulation 6 the RMC fitted datasets and the resulting pair correlation functions are shown in

figures 1 and 2 respectively. Bond lengths can be obtained by gauss fitting the first peak in the pair correlation functions and the second neighbor distances can be obtained in the same manner by fitting the second peak. The bond lengths and second neighbor distances obtained from all simulations are very similar, which indicates that they are well defined by the data. For simulations 1 and 6 they are shown exemplarily in table 4. The observed second neighbor distances support the assumption of corner sharing tetrahedral configurations for Ga and Ge, which can be deduced by simple trigonometric calculations.
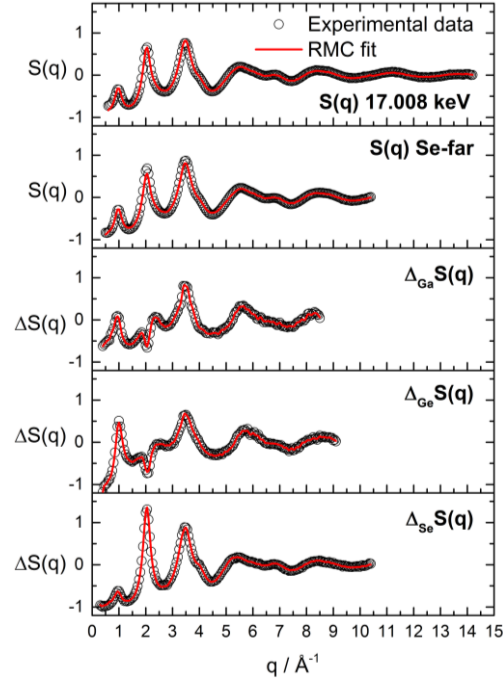

Fig. 1. Experimental structure factors and RMC fits for simulation 6.

In all presented simulations the second neighbor peak in the Ga-Ga pair correlation function has the highest amplitude of all element pairs (see Fig. 2). This means there is a preference for Ga atoms to be located close to each other forming Ga-Se-Ga bonds. The incorporation of Ga into chalcogenide glasses was shown to increase the solubility of rare earth elements.[20,21] Clustering of Ga atoms in the glass structure may provide sites where rare earth atoms can be stabilized by excessive negative charges thus explaining the increased solubility. Similar findings are reported for Ga doped Sulphur-based glasses by Lee et. al.[22]

Table 3. First and second neighbor distances in simulations 1 and 6.

correlation	first neighbor distance / Å		second neighbor distance / Å	
Sim No.	1	6	1	6
Ga-Ga	2.43	-	3.76	3.75
Ga-Ge	2.41	2.40	3.64	3.67
Ga-Se	2.41	2.42	3.93	3.94
Ge-Ge	2.36	-	3.68	3.66
Ge-Se	2.37	2.36	3.85	3.87
Se-Se	2.37	2.38	3.89	3.89

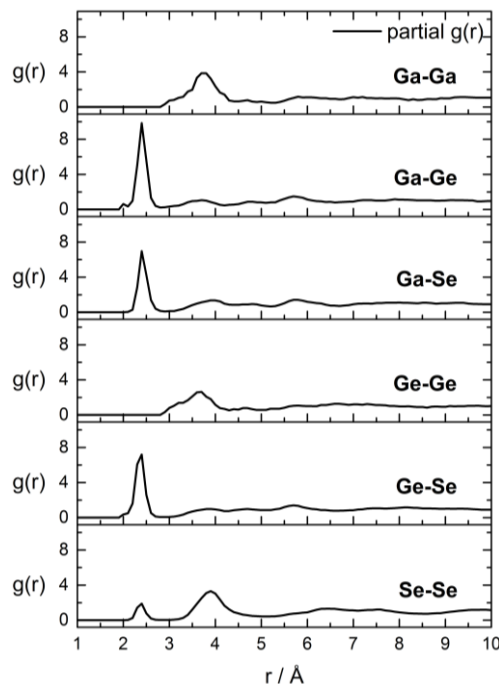*Fig. 2. Partial pair correlation functions from simulation 6*

4. Conclusion

The structure of glassy $(Ga_2Se_3)_{0.25}(GeSe_2)_{0.75}$ was investigated by anomalous X-ray scattering combined with reverse Monte-Carlo modelling featuring increased contrast between the contained elements. It is shown that both gallium and germanium are 4-fold coordinated while selenium has a coordination number greater than 2. These findings are in accordance with previous publications on similar substances. [7-11,23] The local and intermediate range structure around Ga and Ge are almost identical and the presence of wrong bonds for both Ga and Ge is mandatory to reproduce the experimental data. There is no evidence that certain bonds are not present in the material. Furthermore a preference for Ga clustering on a second neighbor length scale is observed which hints at segregation on an intermediate range scale.

References

[1] A. Zakery, S. R. Elliott, Journal of Non-Crystalline Solids **330**, 1(2003).
[2] B. Bureau, X. H. Zhang, F. Smektala, J.-L. Adam, J. Troles, H.-l. Ma, C. Boussard-Plédel, J. Lucas, P. Lucas, D. Le Coq, M. R. Riley, J. H. Simmons, Non-Crystalline Solids **345-346**, 276(2004).
[3] L. Calvez, P. Lucas, M. Rozé, H. L. Ma, J. Lucas, X. H. Zhang, Appl. Phys. A: Mater. Sci. Process. **89**(1), 183(2007).

[4] Y. Nedeva, T. Petkova, E. Mytilineou, P. Petkov, J. Optoelectron. Adv. M. **3**(2), 433(2001).

[5] V. K. Tikhomirov, J. Non-Cryst. Solids **257**, 328(1999).

[6] D. Lezal, J. Optoelectron. Adv. M. **5**, 23(2003).

[7] R. Golovchak, L. Calvez, E. Petracovschi, B. Bureau, D. Savytskii, H. Jain , Materials Chemistry and Physics **138**, 909 (2013).

[8] I. Pethes, R. Chahal, V. Nazabal, C. Prestipino, A. Trapananti, C. Pantalei, B. Beuneu, B. Bureau, P. Jóvári, Journal of Alloys and Compounds **651**, 578 (2015).

[9] [e] A. Mao, D. C. Kaseman, R. E. Youngman, B. G. Aitken, S. Sen, Journal of Non-Crystalline Solids **375**, 40(2013).

[10] A. W. Mao, B. G. Aitken, R. E. Youngman, D. C. Kaseman, S. Sen, J. Phys. Chem. B **117**, 16594(2013).

[11] A. W. Mao, D. C. Kaseman, I. Hung, Z. Gan, B. G. Aitken, S. Sen, Journal of Non-Crystalline Solids **410**, 14 (2015).

[12] J. R. Stellhorn, S. Hosokawa, W.-C. Pilgrim, N. Blanc, N. Boudet, H. Tajiri, S. Kohara, Phys. Status Solidi B **253**(6), 1038 (2016).

[13] W.-C. Pilgrim, J. R. Stellhorn, S. Hosokawa, Bunsen Magazin **15**(3), 131(2013).

[14] S. Hosokawa, I. Oh, M. Sakurai, W.-C. Pilgrim, N. Boudet, J.-F. Bérar, S. Kohara, Phys. Rev. B **84**, 014201(2011).

[15] Y. Waseda, "Novel Application of Anomalous X-ray Scattering for Structural Characterization of Disordered Materials", Springer-Verlag, Heidelberg, 1984.

[16] J.R. Stellhorn, S. Hosokawa, W.-C. Pilgrim, Z. Phys. Chem. **228**(10–12) 1005(2014).

[17] O. Gereben, P. Jóvári, L. Temleitner, L. Pusztai, J. Optoelectron. Adv. M. **9**, 3021(2007).

[18] https://www.szfki.hu/~nphys/rmc++/RMC_POT_user_guide.pdf.

[19] A. Kjekshus, Acta Chemica Scandinavia **18**, 2379(1964).

[20] M. Scheffler, J. Kirchhof, J. Kobelke, K. Schuster, A. Schwuchow, Journal of Non-Crystalline Solids **256-257**, 59(1999).

[21] Y. G. Choi, K. H. Kim, B. J. Lee, Y. B. Shin, Y. S. Kim, J. Heo, Journal of Non-Crystalline Solids **278**, 137(2000).

[22] T. H. Lee, S. I. Simdyankin, J. Hegedus, J. Heo, S. R. Elliott, Phys. Rev. B **81**, 104204(2010).

[23] K. Maeda, T. Sakai, K. Sakai, T. Ikari, M. Munzar, D. Tonchev, S. O. Kasap, G. Lucovsky, J. Mater. Sci.: Mater. Electron. **18**, 367(2007).